A Letters Journal Exploring the Frontiers of Physics

April 2012

EPL, **98** (2012) 14004
doi: 10.1209/0295-5075/98/14004

www.epljournal.org

Dissipation of micro-cantilevers as a function of air pressure and metallic coating

T. J. Li[1,2] and L. Bellon[1(a)]

[1] *Université de Lyon, Laboratoire de physique, ENS Lyon, CNRS - 46 Allée d'Italie, Lyon 69364, France, EU*
[2] *Department of Physics, East China Normal University - 3663 Zhongshan North Rd., Shanghai 200062, China*

received 30 October 2011; accepted in final form 9 March 2012
published online 12 April 2012

PACS 46.35.+z – Viscoelasticity, plasticity, viscoplasticity
PACS 05.40.Jc – Brownian motion
PACS 07.10.Cm – Micromechanical devices and systems

Abstract – In this letter, we characterize the internal dissipation of coated micro-cantilevers through their mechanical thermal noise. Using a home-made interferometric setup, we achieve a resolution down to $10^{-14}\,\mathrm{m}\sqrt{\mathrm{Hz}}$ in the measurement of their deflection. With the use of the fluctuation dissipation theorem and of the Kramers-Kronig relations, we rebuild the full mechanical response function from the measured noise spectrum, and investigate frequency-dependent dissipation as a function of the air pressure and of the nature of the metallic coatings. Using different thicknesses of gold coatings, we demonstrate that the internal viscoelastic damping is solely due to the dissipation in the bulk of the coating.

Microsized cantilevers are present in many applications, ranging from chemical and biological sensors [1] to atomic force microscopy (AFM) [2]. They are also used as a basic brick for microelectromechanical systems (MEMS). As mass detectors, for example, they can be functionalized for the adsorption of specific chemical compounds by proper coating of their surface: the mass increment is detected as a resonance frequency shift. Gold coating is widely used due to the large selection of materials that can be adsorbed via thiol chemistry [1,3]. Besides, from a gold layer, electrically conducting layers can be patterned and integrated into the cantilever for local heating [4], magnetomotive actuation [5] or piezoresistive readout of the deflection [6].

The sensitivity of the resonant cantilever when used as a mass sensor depends on the spectral resolution, thus of its quality factor Q defined as the ratio of stored vibrational energy over energy lost per cycle of vibration [7]. The greatest sensitivity will thus be reached with the smallest dissipation. The functionality of MEMS, AFM probe or mass sensors is based on the deformation of the cantilever. Thermally induced mechanical fluctuations determine the ultimate deflection sensitivity of these sensors and represent one of the most important noise sources. They are linked to the damping of the system, as shown by the fluctuation dissipation theorem (FDT) [8]. Smaller damping will thus lead to reduced thermal noise, thus increasing the sensitivity and usability of the probes. It is therefore of prime importance to understand and characterize the dissipation sources in these systems.

Great effort has been put into describing the effect of ambient pressure and cantilever coating on their resonant behavior, both experimentally [9–17] and theoretically [18–20]. For example, Sandberg [14] investigated the effect of gold coating on the quality factor of a resonant cantilever and showed that in vacuum Q is severely reduced by the deposition of even a thin gold film (100 nm), especially for higher-order modes. Considering only structural damping, Saulson [18] proposed a viscoelastic model, in which the power spectrum density (PSD) of thermal induced deflection presents a characteristic $(1/f)$-like trend. In a previous work [15], we introduced a simple power law to describe the frequency dependence of this viscoelasticity on a gold coated cantilever, and a model that includes Sader's approach to describe the coupling with the surrounding atmosphere [20,21]. We showed that the damping is only due to the coating when viscous dissipation vanishes in vacuum. Understanding the source of this coating induced viscoelasticity will undoubtedly help in designing more sensitive and accurate cantilever based sensors and microprobes. However, measuring the thermal noise or small damping over a wide

(a) E-mail: Ludovic.Bellon@ens-lyon.fr

range of frequencies is a great challenge, and very few experiments [15,21–24] have succeeded so far in directly measuring fluctuations out of resonance, notably at low frequency.

In this work, we measure the thermal noise of AFM cantilevers, with a highly sensitive interferometric technique [15,21], allowing access to the whole spectrum from 1 Hz to 20 kHz with a background noise as low as $10^{-28}\,\mathrm{m}^2/\,\mathrm{Hz}$ (see fig. 1). With the use of the FDT and of the Kramers-Kronig relations, we rebuild the full mechanical response function from the measured PSD [15]. We can therefore characterize dissipation of micro-cantilevers as a function of the air pressure and of the metallic coatings. Let us first briefly recall the theoretical background for our analysis of thermal noise, before describing the experiments and concluding with a discussion on the results.

Since our cantilevers are in equilibrium at temperature T, the thermal fluctuations of their deflection d are described by the FDT, relating the PSD to the mechanical response function G of the system:

$$S_d(f) = -\frac{4k_BT}{\omega}\mathrm{Im}\left[\frac{1}{G(\omega)}\right], \qquad (1)$$

where k_B is the Boltzmann constant, $\omega = 2\pi f$ the pulsation corresponding to frequency f, and Im stands for the imaginary part of its argument. $G(\omega)$ is defined in the Fourier space as $G(\omega) = F(\omega)/d(\omega)$, where F is the force coupled to d in the Hamiltonian of the system. Considering both internal and viscous damping [7,15,18], we have

$$G(\omega) = k\left[1 - \frac{\omega^2}{\omega_0^2} + i\left(\frac{\omega}{\omega_0 Q_a} + \phi\right)\right] \qquad (2)$$

with $k^* = k(1 + i\phi)$ the complex spring constant, ω_0 the resonant pulsation and Q_a the quality factor linked to viscous damping in air. The internal damping is described generically by ϕ, and may have several sources: clamping and support losses, viscoelasticity, surface losses, thermoelastic dissipation (TED), etc. At resonance, we observe an effective quality factor Q_{eff} defined as

$$\frac{1}{Q_{\mathrm{eff}}} = \frac{1}{Q_a} + \phi. \qquad (3)$$

In the experiments, it is hard to characterize dissipation outside resonance: the imaginary part of G is much smaller than its real part, and the forcing method has to be perfectly controlled to perform such measurement. We therefore use the FDT (eq. (1)) to infer $\mathrm{Im}[1/G(\omega)]$ from the measurement of the thermal noise S_d, then Kramers-Kronig integral relations to rebuild the full mechanical response function G from the knowledge of this imaginary part. Using this method, we have shown that both Q_a and ϕ are in fact weakly frequency dependent for the model to match the experimental observations [15]. $Q_a(\omega)$ is described by Sader's approach for viscous damping [20], and the internal damping is following a simple power law with a small exponent: $\phi(\omega) \propto \omega^\alpha$, with $\alpha \approx -0.11$ for a commercial gold coated cantilever [15]. In this letter,

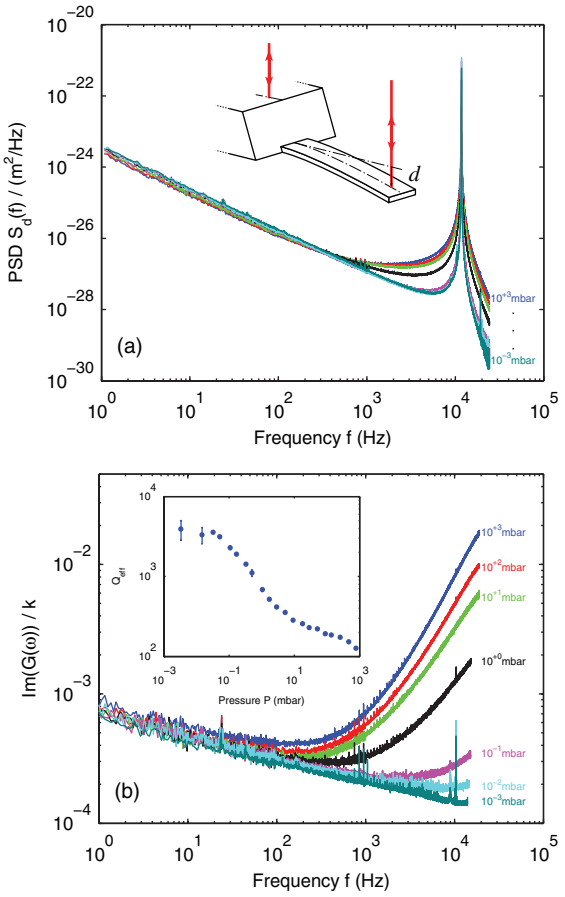

Fig. 1: (Colour on-line) (a) Thermal noise spectrum and (b) reconstructed dissipative part of the response function G of cantilever **cAu** at different pressures. Background noise due to the electronics has been subtracted from the measured PSD. Viscous damping, dominant at high frequency and high pressure over internal dissipation, vanishes in vacuum, leading to a sharper resonance. The inset in (a) illustrates our high precision interferometric method: interferences between beams reflecting on the base and free extremity of the cantilever directly measure its deflection d [15,25]. Inset in (b): effective quality factor Q_{eff} at resonance as a function of pressure.

we demonstrate how viscous damping vanishes when the pressure decreases, and characterize the behavior of ϕ for different coatings.

We use silicon AFM cantilevers with the following geometry: length $450 \pm 10\,\mu$m, width $50 \pm 5\,\mu$m, thickness $2 \pm 1\,\mu$m. Their resonant frequency is around 13 kHz. We present here characteristic data corresponding to three types of AFM cantilevers (around 10 samples were measured for each type), which properties are summarized in table 1. In addition, we performed successive gold layer depositions on three other types of probe, also detailed in table 1. Layer thickness increments were around 10 nm for the first 3 evaporations, then around 20 nm. Cantilever **dSi** is initially a raw silicon cantilever, prepared with a 2 nm Cr adhesion layer before deposition. Its initial internal friction is too small to be measured with our precision.

Table 1: Sets of cantilevers characterized in the experiments. For cantilevers where we performed additional gold depositions, layer thickness increments were around 10 nm for the first 3 evaporations, then around 20 nm.

Cantilever	Commercial type	Adhesion layer	Initial coating	Additional gold coating
cAu	Budget sensors (ContGB)	2×5 nm Cr	2×70 nm Au	–
cPt	Nanoworld POINTPROBE (ContPt-50)	2×5 nm Cr	2×23 nm PtIr	–
cAl	Budget sensors (BS-ContAl)	2×5 nm Cr	1×30 nm Al	–
dAu	Budget sensors (ContGB)	2×5 nm Cr	2×70 nm Au	$10\,\text{nm} + 10\,\text{nm} + \ldots$
dPt	Nanoworld POINTPROBE (ContPt-50)	2×5 nm Cr	2×23 nm PtIr	$10\,\text{nm} + 10\,\text{nm} + \ldots$
dSi	Budget sensors (All In One-TL)	1×2 nm Cr	–	$10\,\text{nm} + 10\,\text{nm} + \ldots$

In the spectra presented in fig. 1(a), the $(1/f)$-like noise is the clear signature of the internal dissipation of the cantilever. In our preliminary work [15], we checked in various ways that this measurement is linked only to the thermal mechanical noise of the cantilever, and not to any spurious detection artifact: the interferometer background noise is more than one order of magnitude below the measured values (except for a raw silicon cantilever in vacuum, for which only the thermal noise at resonance can be measured), and 3 independent tests have been performed to rule out possible coupling with the laser intensity fluctuations evidenced in [26].

We first study the influence of ambient pressure P on cantilever **cAu**. In fig. 1, we plot the PSD of the deflection for different pressures from ambient to 10^{-3} mbar, and the corresponding reconstructed response function (imaginary part only, normalized by spring constant k). Dissipation is clearly the sum of two contribution: pressure-independent internal damping $\phi(\omega)$, always dominant at low frequency, and viscous damping term $\omega/\omega_0 Q_a(\omega)$, dominant at high frequency and high pressure, but vanishing in vacuum. At resonance, the effective quality factor thus increases when the pressure drops, but saturates to a finite value due to the internal dissipation. For this cantilever and the frequency range probed here, viscous damping becomes negligible when $P < 10^{-2}$ mbar. In vacuum, the dissipative part of the response function directly leads to the internal dissipation: $\phi(\omega) = \text{Im}[G(\omega)]/k$ when $Q_a \to \infty$. A simple power law matches well the observed frequency dependence [15], with an exponent $\alpha_{\text{Au}} \approx -0.15$.

To check the generic validity of this behavior, we measure in vacuum the internal damping of different metallic coatings, and report the results for cantilevers **cAu**, **cPt** and **cAl** in fig. 2. The magnitude of this dissipation is smaller for the 2 other coatings, but the weak frequency dependence is a common characteristic. At high frequency (above 1 kHz), the viscous damping is still observable for cantilever **cPt** at the lowest pressure achievable in our system (10^{-3} mbar). If we limit the frequency range to 1 kHz for this sample, we observe a similar power-law dependence with an exponent $\alpha_{\text{Pt}} \approx -0.12$. The data of the last cantilever, **cAl**, is a little bit different with a very flat measurement, leading to $\alpha_{\text{Al}} \approx 0$. The power-law dependence thus works generically, though the exponent changes slightly for each cantilever.

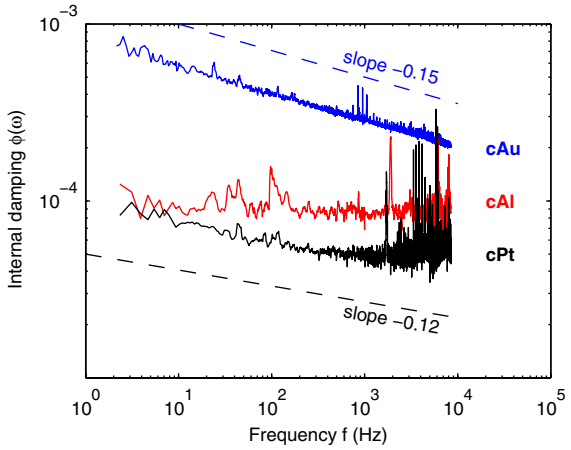

Fig. 2: (Colour on-line) Internal damping $\phi(\omega)$ of cantilevers **cAu**, **cAl** and **cPt** reconstructed from the noise spectrums measured in vacuum.

To investigate the origin of this internal damping, we finally measured this quantity for cantilevers **dSi**, **dPt** and **dAu** as a function of the thickness h_c of an added gold coating: the same 3 cantilevers where characterized in vacuum between successive layers deposition, and we plot in fig. 3 the value of the dissipation at low frequency (average value of $\phi(\omega)$ between 100 Hz and 200 Hz) and at resonance (value of $1/Q_{\text{eff}}$, deduced from a Lorenzian fit of the PSD). Internal dissipation is roughly proportional to the thickness, and remains weakly frequency dependent in these observations. This behavior suggests that the main contribution to the internal damping of the cantilever originates in the bulk of the coating, rather than from a surface or interface effect. Indeed, if such phenomenon was dominant, it would be present even for the lowest thickness, whereas we observe a vanishing dissipation when the coating layer gets thinner. Moreover, the value of the dissipation is independent of the adhesion layer for the gold coating: we get the same results for 2 nm of Cr (cantilever **dSi**) and for 23 nm of PtIr5 (cantilever **dPt**).

To understand the mechanism of this internal damping, let us estimate the contribution of the main sources of dissipation (discarding viscous damping by air which as already been characterized and is negligible in

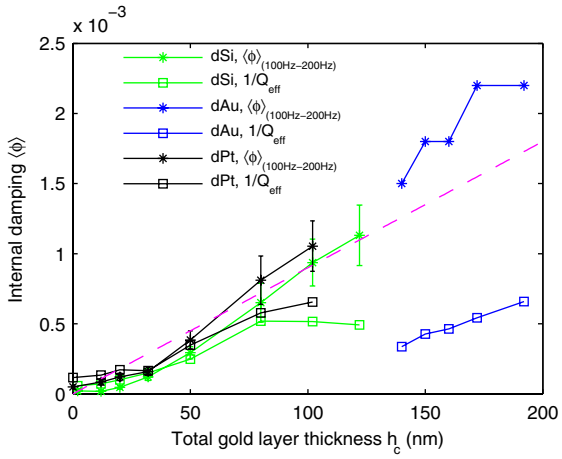

Fig. 3: (Colour on-line) Internal damping at low and high frequency (average of $\phi(\omega)$ around 150 Hz and $1/Q_{\rm eff}$ at resonance) as a function of the total gold layer thickness for cantilevers **dSi**, **dAu** and **dPt**. Typical error bars (dispersion over a few acquisitions) are shown for two cantilevers. The dashed line corresponds to a linear dependence of ϕ in gold thickness h_c, expected if the viscoelasticity of the coating is the only relevant damping process.

vacuum) [17]:

$$\phi = \phi_{\rm clamping} + \phi_{\rm support} + \phi_{\rm TED} + \phi_{\rm internal} + \phi_{\rm coating} + \phi_{\rm surface}, \quad (4)$$

where each term in this sum corresponds, respectively, to clamping and support losses, thermoelastic dissipation (TED), other source of internal dissipation inside the bulk of cantilever (often called internal friction or viscoelasticity), dissipation inside the bulk of the coating, and all surfaces and interfaces contributions to damping. Let us now discuss each of these terms to extract the relevant ones.

– $\phi_{\rm clamping}$: the cantilever and its chip are fabricated in a monolithic design, the clamping loss can thus be largely minimized. The related dissipation can be estimated by equation $\phi_{\rm clamping} \sim (h/l)^3$ [27], where l and h are the length and the thickness of the cantilever. In our geometry ($l = 450\,\mu$m, $h = 2\,\mu$m) this loss is of the order of 10^{-7}, and thus negligible.

– $\phi_{\rm support}$: thanks to our well-designed cantilever holder, the support loss is also negligible. As a simple illustration of this fact, the total dissipation of a raw silicon cantilever in vacuum is not measurable outside resonance, with an upper bound around 10^{-5}.

– $\phi_{\rm TED}$: for a silicon cantilever, thermoelastic damping can be estimated by [28]

$$\phi_{\rm TED} = \frac{E\beta^2 T}{C}\frac{\Omega}{1+\Omega^2}, \quad (5)$$

where $E = 169$ GPa is Young's modulus of silicon, $\beta = 2.6 \times 10^{-6}\,{\rm K}^{-1}$ its linear coefficient of thermal expansion, $C = 2.6 \times 10^6\,{\rm J\cdot m^{-3}\,K^{-1}}$ its specific heat per unit volume and Ω the normalized frequency defined as

$$\Omega = \omega\frac{Ch^2}{\pi^2\lambda}, \quad (6)$$

where $\lambda = 149\,{\rm W\cdot m^{-1}\,K^{-1}}$ is the thermal conductivity. In our case, $h = 2\,\mu$m, $\omega = 2\pi f < 2 \times 10^5$ rad/s, leading to $\phi_{\rm TED} < 10^{-6}$, below our precision level. Using values from [29], we checked that the change in TED due to metallization was also not meaningful in our experiment.

– $\phi_{\rm internal}$: we use commercially available high-quality monocrystal silicon cantilevers, thus the bulk loss (internal friction) caused by the motion of crystallographic defects is negligible. Again, as a simple illustration of this fact, the total dissipation of a raw silicon cantilever in vacuum is not measurable outside resonance, with an upper bound around 10^{-5}.

– $\phi_{\rm coating}$: this contribution corresponds to the internal dissipation in the bulk of the coating, and is estimated by [7,17]

$$\phi_{\rm coating} = 3\frac{E_{\rm c}}{E}\frac{h_c}{h}\phi_{\rm c}, \quad (7)$$

where $E_{\rm c}$, $\phi_{\rm c}$ and h_c are bulk Young's modulus, bulk viscoelasticity and thickness of the coating layer (index c). This contribution is thus proportional to the layer thickness h_c.

– $\phi_{\rm surface}$: this last contribution accounts for the processes of dissipation that may occur at the surface of the cantilever and the interfaces between the silicon cantilever and the various coating layers. By definition, this terms should be independent of the thickness of the coating layer.

Within our experimental precision, all terms in the sum of eq. (4) but the two last ones are negligible, so the total dissipation in vacuum is

$$\phi = \phi_{\rm surface} + 3\frac{E_{\rm c}}{E}\frac{h_c}{h}\phi_{\rm c}. \quad (8)$$

As illustrated in fig. 3, total dissipation in the case of a gold coating is simply proportional to the thickness h_c, thus $\phi_{\rm surface}$ is negligible in our experiments. The dissipation that we measure is therefore solely due to the viscoelastic properties of the bulk of the coating, and proportional to h_c.

Using manufacturer values for metallic layers of cantilevers **cAu**, **cAl** and **cPt**, we can thus extract the viscoelasticity $\phi_{\rm c}$ of each coating from the measurement of the total dissipation ϕ, and plot the result in fig. 4. PtIr5 is the least dissipative material, with a damping about an order of magnitude lower than gold or aluminum. Those two last materials have similar viscoelasticity, aluminum

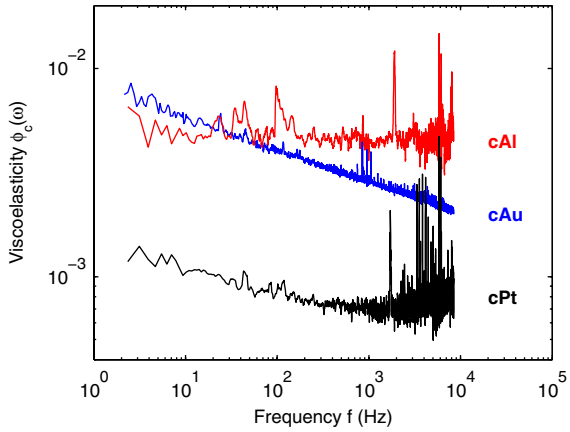

Fig. 4: (Colour on-line) Intrinsic viscoelasticity ϕ_c of gold, aluminum and PtIr5 coatings (corresponding to cantilevers **cAu**, **cAl** and **cPt**) as a function of frequency.

being better at low frequency (below ∼50 Hz) and worse above. Obviously these internal dampings within coatings still follow the same simple power law as described before. The results agree reasonably with the work of Sosale and collaborators [17] in the smaller frequency range probed in their experiments on gold and aluminum.

As a conclusion, let us summarize the main points illustrated in this letter. We measure the thermal noise of AFM cantilevers with a high-resolution interferometer, and reconstruct from this data their dissipation. The damping of coated cantilevers is shown to arise from two distinct sources: viscous damping due to the external atmosphere, dominant at high frequency and ambient pressure, and internal viscoelastic damping, dominant at low frequency or in vacuum. This viscoelasticity is linked to the presence of a coating on the cantilever, and can be modeled by a complex spring constant. This dissipation is accurately fitted by a simple power law ω^α on up to 4 decades in frequency, with a small exponent α depending on coating material and procedure: for the cantilevers probed here, $\alpha_{\rm Au} \approx -0.15$, $\alpha_{\rm Pt} \approx -0.12$, and $\alpha_{\rm Al} \approx 0$. Changing the coating thickness, we show that this dissipation is due to the bulk of the coating rather than to some interface friction between layers, and extract the intrinsic viscoelasticity for each material. Damping increases by one order of magnitude between PtIr5 and gold or aluminum coating.

These results demonstrate that the choice of the coating material is critical with respect to internal dissipation in micro-cantilevers, and that gold (or aluminum) are actually not the best with respect to this criterion. If this material is however required for its chemical properties, using the lowest functional thickness is advisable to minimize damping.

Our characterization procedure features an excellent resolution with measurement of overall mechanical loss tangents down to 10^{-4}. This way, the viscoelasticity due to the coating can be accurately quantified and our measurements should be useful in the perspective of testing models of internal friction, eventually leading to improved coating procedures and better performance of cantilever based sensors. Our method would also be suited to study other type of coatings, such as those implied in chemical or biological sensors, alone or linked to the target molecules.

* * *

We thank F. Vittoz and F. Ropars for technical support, and S. Ciliberto, A. Petrosyan and C. Fretigny for stimulating discussions.

REFERENCES

[1] Lavrik N. V., Sepaniak M. J. and Datskos P. G., *Rev. Sci. Instrum.*, **75** (2004) 2229.
[2] Meyer E., Hug H. J. and Bennewitz R., *Scanning Probe Microscopy: The Lab on a Tip* (Springer) 2004.
[3] Ziegler C., *Anal. Bioanal. Chem.*, **379** (2004) 946.
[4] Ataka M., Omodaka A., Takeshima N. and Fujita H., *J. Microelectromech. Syst.*, **2** (1993) 146.
[5] Lange D., Hagleitner C., Herzog C., Brand O. and Baltes H., *Magnetic actuation and MOS-transistor sensing for CMOS-integrated resonators*, in *The 15th IEEE International Conference on Micro Electro Mechanical Systems* (IEEE Conference Publications) 2002, DOI: 10.1109/MEMSYS.2002.984263, pp. 304–307.
[6] Rasmussen P. A., Thaysen J., Hansen O., Eriksen S. C. and Boisen A., *Ultramicroscopy*, **97** (2003) 371.
[7] Yasumura K. Y., Stowe T. D., Chow E. M., Pfafman T., Kenny T. W., Stipe B. C. and Rugar D., *J. Microelectromech. Syst.*, **9** (2000) 117.
[8] Callen H. B. and Greenet R. F., *Phys. Rev.*, **86** (1952) 702.
[9] Bergaud C., Nicu L. and Martinez A., *Jpn. J. Appl. Phys.*, **38** (1999) 6521.
[10] Chon J. W. M., Mulvaney P. and Sader J. E., *J. Appl. Phys.*, **87** (2000) 3978.
[11] Yang J., Ono T. and Esashi M., *J. Microelectromech. Syst.*, **11** (2002) 775.
[12] Yum K., Wang Z., Suryavanshi A. P. and Yu M.-F., *J. Appl. Phys.*, **96** (2004) 3933.
[13] Sandberg R., Molhave K., Boisen A. and Svendsen W., *J. Micromech. Microeng.*, **15** (2005) 2249.
[14] Sandberg R., Svendsen W., Lhave K. M. and Boisen A., *J. Micromech. Microeng.*, **15** (2005) 1454.
[15] Paolino P. and Bellon L., *Nanotechnology*, **20** (2009) 405705.
[16] Lubbe J., Troger L., Torbrugge S., Bechstein R., Richter C., Kuhnle A. and Reichling M., *Meas. Sci. Technol.*, **21** (2010) 125501.
[17] Sosale G., Prabhakar S., Frechette L. and Vengallatore S., *J. Microelectromech. Syst.*, **20** (2011) 764.
[18] Saulson P. R., *Phys. Rev. D*, **42** (1990) 2437.
[19] Leveque G., Girard P., Belaidi S. and Cohen G. S., *Rev. Sci. Instrum.*, **68** (1997) 4137.

[20] Sader J. E., *J. Appl. Phys.*, **84** (1998) 64.
[21] Bellon L., *J. Appl. Phys.*, **104** (2008) 104906.
[22] Numata K., Ando M., Yamamoto K., Otsuka S. and Tsubono K., *Phys. Rev. Lett.*, **91** (2003) 260602.
[23] González G. I. and Saulson P. R., *Phys. Lett. A*, **201** (1995) 12.
[24] Kajima M., Kusumi N., Moriwaki S. and Mio N., *Phys. Lett. A*, **263** (1999) 21.
[25] Schonenberger C. and Alvarado S. F., *Rev. Sci. Instrum.*, **60** (1989) 3131.
[26] Labuda A., Bates J. R. and Grütter P. H., *Nanotechnology*, **23** (2012) 025503.
[27] Hosaka H., Itao K. and Kuroda S., *Sens. Actuators A: Phys.*, **49** (1995) 87.
[28] Zener C., *Phys. Rev.*, **53** (1938) 90.
[29] Vengallatore S., *J. Micromech. Microeng.*, **15** (2005) 2398.